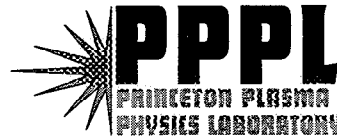


# 3D Multispecies Nonlinear Perturbative Particle Simulations of Two-Stream Instabilities in Intense Particle Beams

Hong Qin, Ronald C. Davidson, and W. Wei-li Lee  
Plasma Physics Laboratory  
Princeton University



Presented at  
8th ICFA Beam Dynamics Mini-Workshop  
on Two-Stream Instabilities  
Santa Fe, New Mexico, February 16 – 18, 2000

---

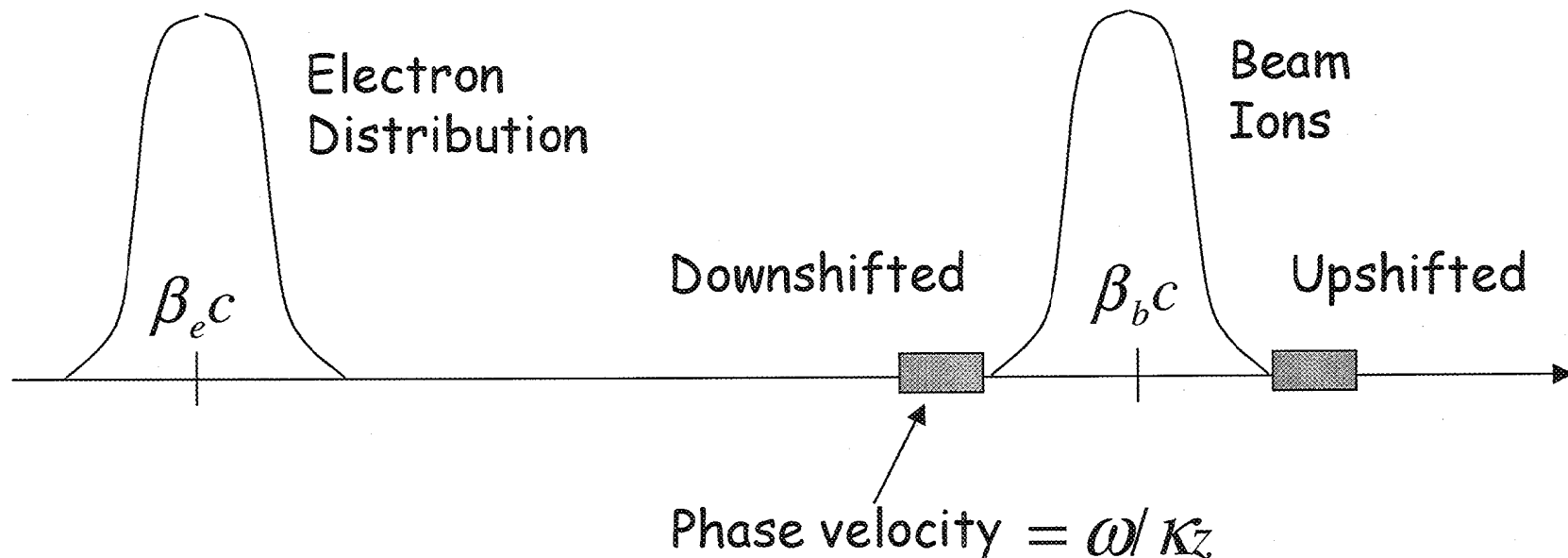
\*Research supported by the U.S. Department of Energy, the Short Pulse Spallation Source project and LANSCE Division of Los Alamos National Laboratory, and the Spallation Neutron Source project.

- ⇒ Understand two-stream interaction process in high-intensity ion beams, and identify optimum operating regimes for:
  - Spallation neutron sources.
  - Hadron colliders.
  - Heavy ion fusion.
  
- ⇒ 3D multi-species nonlinear  $\delta f$  particle simulation code provides an effective tool for investigating the following processes:
  - Electron-ion two-stream instability.
  - Nonlinear dynamics of collective interaction processes.
  - Periodically-focused beam propagation in alternating-gradient focusing fields.

- ⇒ Theoretical model — nonlinear Vlasov-Maxwell system
- ⇒ Solution method — 3D perturbative ( $\delta f$ ) particle simulation
- ⇒ e-p instability — mode structure, growth rate, and stabilization mechanism
- ⇒ Conclusions

## Two-Stream Instability for Intense Ion Beam

- ⇒ In the absence of background electrons, an intense nonneutral ion beam supports collective oscillations (plasma oscillations) with phase velocity  $\omega/k_z$  upshifted and downshifted relative to the average beam velocity  $\beta_b c$ .
- ⇒ Introduction of an (unwanted) electron component (produced, for example, by secondary emission of electrons due to the interaction of halo ions with the chamber wall) provides the free energy to drive the classical two-stream instability.



- ⇒ Thin, continuous, high-intensity ion beam ( $j = b$ ) propagates in the  $z$ -direction through background electron and ion components ( $j = e, i$ ) described by distribution function  $f_j(\mathbf{x}, \mathbf{p}, t)$ .
- ⇒ Transverse and axial particle velocities in a frame of reference moving with axial velocity  $\beta_j c \hat{\mathbf{e}}_z$  are assumed to be *nonrelativistic*.
- ⇒ Adopt a *smooth-focusing* model in which the focusing force is described by

$$\mathbf{F}_j^{foc} = -\gamma_j m_j \omega_{\beta j}^2 \mathbf{x}_\perp$$

- ⇒ Self-electric and self-magnetic fields are expressed as  $\mathbf{E}^s = -\nabla\phi(\mathbf{x}, t)$  and  $\mathbf{B}^s = \nabla \times A_z(\mathbf{x}, t) \hat{\mathbf{e}}_z$ .

⇒ Distribution functions and electromagnetic fields are described self-consistently by the nonlinear Vlasov-Maxwell equations in the six-dimensional phase space  $(\mathbf{x}, \mathbf{p})$ :

$$\left\{ \frac{\partial}{\partial t} + \mathbf{v} \cdot \frac{\partial}{\partial \mathbf{x}} - \left[ \gamma_j m_j \omega_{\beta j}^2 \mathbf{x}_{\perp} + e_j (\nabla \phi - \frac{v_z}{c} \nabla_{\perp} A_z) \right] \cdot \frac{\partial}{\partial \mathbf{p}} \right\} f_j(\mathbf{x}, \mathbf{p}, t) = 0$$

and

$$\begin{aligned} \nabla^2 \phi &= -4\pi \sum_j e_j \int d^3 p f_j(\mathbf{x}, \mathbf{p}, t) \\ \nabla^2 A_z &= -\frac{4\pi}{c} \sum_j e_j \int d^3 p v_z f_j(\mathbf{x}, \mathbf{p}, t) \end{aligned}$$

- ⇒ Divide the distribution function into two parts:  $f_j = f_{j0} + \delta f_j$  .
- ⇒  $f_{j0}$  is a known solution to the nonlinear Vlasov-Maxwell equations.
- ⇒ Determine numerically the evolution of the perturbed distribution function  $\delta f_j \equiv f_j - f_{j0}$  .
- ⇒ Advance the weight function defined by  $w_j \equiv \delta f_j / f_j$ , together with the particles' positions and momenta.
- ⇒ Equations of motion for the particles are given by

$$\begin{aligned} \frac{d\mathbf{x}_{ji}}{dt} &= (\gamma_j m_j)^{-1} \mathbf{p}_{ji} \\ \frac{d\mathbf{p}_{ji}}{dt} &= -\gamma_j m_j \omega_{\beta j}^2 \mathbf{x}_{\perp ji} - e_j \left( \nabla \phi - \frac{v_{zji}}{c} \nabla_{\perp} A_z \right) \end{aligned}$$

- ⇒ Weight functions  $w_j$  are carried by the simulation particles, and the dynamical equations for  $w_j$  are derived from the definition of  $w_j$  and the Vlasov equation.

⇒ Weight functions evolve according to

$$\begin{aligned} \frac{dw_{ji}}{dt} &= -(1 - w_{ji}) \frac{1}{f_{j0}} \frac{\partial f_{j0}}{\partial \mathbf{p}} \cdot \delta \left( \frac{d\mathbf{p}_{ji}}{dt} \right) \\ \delta \left( \frac{d\mathbf{p}_{ji}}{dt} \right) &\equiv -e_j \left( \nabla \delta \phi - \frac{v_{zji}}{c} \nabla_{\perp} \delta A_z \right) \end{aligned}$$

Here,  $\delta \phi = \phi - \phi_0$ ,  $\delta A_z = A_z - A_{z0}$ , and  $(\phi_0, A_{z0}, f_{j0})$  are the equilibrium solutions.

⇒ The perturbed distribution function  $\delta f_j$  is given by the weighted Klimontovich representation

$$\delta f_j = \frac{N_j}{N_{sj}} \sum_{i=1}^{N_{sj}} w_{ji} \delta(\mathbf{x} - \mathbf{x}_{ji}) \delta(\mathbf{p} - \mathbf{p}_{ji})$$

where  $N_j$  is the total number of actual  $j$ 'th species particles, and  $N_{sj}$  is the total number of *simulation* particles for the  $j$ 'th species.



⇒ Maxwell's equations are also expressed in terms of the perturbed quantities:

$$\begin{aligned}\nabla^2 \delta\phi &= -4\pi \sum_j e_j \delta n_j \\ \nabla^2 \delta A_z &= -\frac{4\pi}{c} \sum_j \delta j_{zj} \\ \delta n_j &= \int d^3 p \delta f_j(\mathbf{x}, \mathbf{p}, t) = \frac{N_j}{N_{sj}} \sum_{i=1}^{N_{sj}} w_{ji} S(\mathbf{x} - \mathbf{x}_{ji}) \\ \delta j_{zj} &= e_j \int d^3 p v_z \delta f_j(\mathbf{x}, \mathbf{p}, t) = \frac{e_j N_j}{N_{sj}} \sum_{i=1}^{N_{sj}} v_{zji} w_{ji} S(\mathbf{x} - \mathbf{x}_{ji})\end{aligned}$$

where  $S(\mathbf{x} - \mathbf{x}_{ji})$  represents the method of distributing particles on the grids.

- ⇒ Simulation noise is reduced significantly.
  - Statistical noise  $\sim 1/\sqrt{N_s}$ .
  - To achieve the same accuracy, number of simulation particles required by the  $\delta f$  method is only  $(\delta f/f)^2$  times of that required by the conventional PIC method.
- ⇒ No waste of computing resource on something already known —  $f_0$ .
- ⇒ Moreover, make use of the known ( $f_0$ ) to determine the unknown ( $\delta f$ ).
- ⇒ Study physics effects separately, as well as simultaneously.
- ⇒ Easily switched between linear and nonlinear operation.

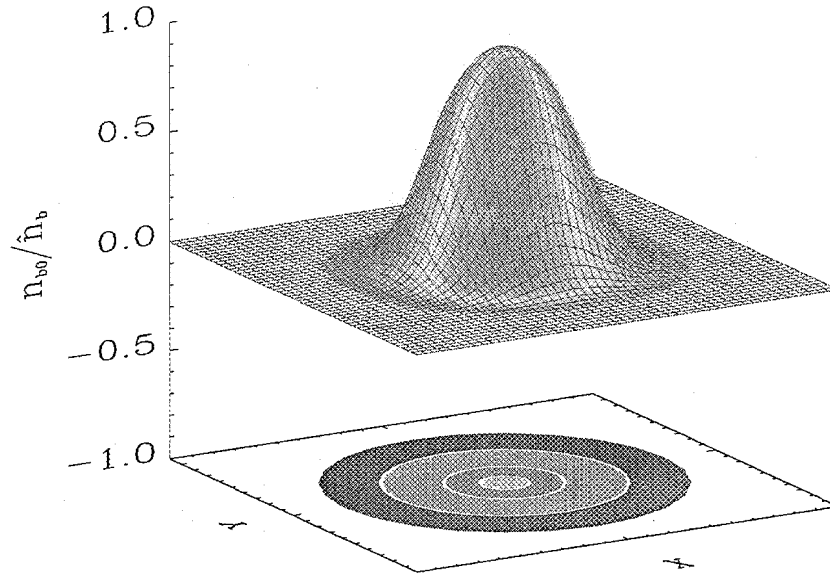
Implementation of the 3D multispecies nonlinear  $\delta f$  simulation method described above is embodied in the Beam Equilibrium Stability and Transport (BEST) code at the Princeton Plasma Physics Laboratory.

- ⇒ Adiabatic field pusher for light particles (electrons).
- ⇒ Solves Maxwell's equations in cylindrical geometry.
- ⇒ Written in Fortran 90/95 and extensively object-oriented.
- ⇒ NetCDF data format for large-scale diagnostics and visualization.
- ⇒ Achieved an average speed of  $40\mu\text{s}/(\text{particle}\times\text{step})$  on a DEC alpha personal workstation 500au computer.
- ⇒ The code is being parallelized using OpenMP and MPI.
- ⇒ Achieved  $20 \times 10^9$  ion-steps +  $100 \times 10^9$  electron-steps for instability studies.

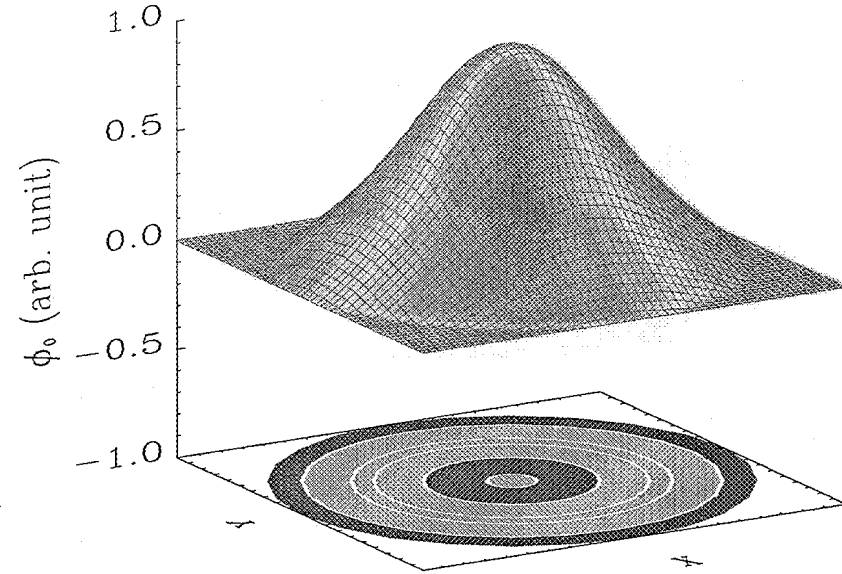
- ⇒ Single-species thermal equilibrium ion beam in a constant focusing field.
- ⇒ Equilibrium properties depend on the radial coordinate  $r = \sqrt{(x^2 + y^2)}$ .
- ⇒ Cylindrical chamber with perfectly conducting wall located at  $r = r_w$ .
- ⇒ Thermal equilibrium distribution function for the beam ion is given by

$$f_{b0}(r, \mathbf{p}) = \frac{\hat{n}_b}{(2\pi\gamma_b m_b T_b)^{3/2}} \exp\left\{-\frac{p_{\perp}^2/2\gamma_b m_b + \gamma_b m_b \omega_{\beta b}^2 r^2/2 + e_b(\phi_0 - \beta_b A_{z0})}{T_b}\right\} \\ \times \exp\left\{-\frac{(p_z - \gamma_b m_b \beta_b c)^2}{2\gamma_b m_b T_b}\right\},$$

- ⇒ In initial benchmark tests, system parameters are chosen to be:  $\gamma_b = 1.05$ ,  $A = 133$  and normalized beam intensity  $\hat{\omega}_{pb}^2/2\gamma_b^2\omega_{\beta b}^2 = 0.9$

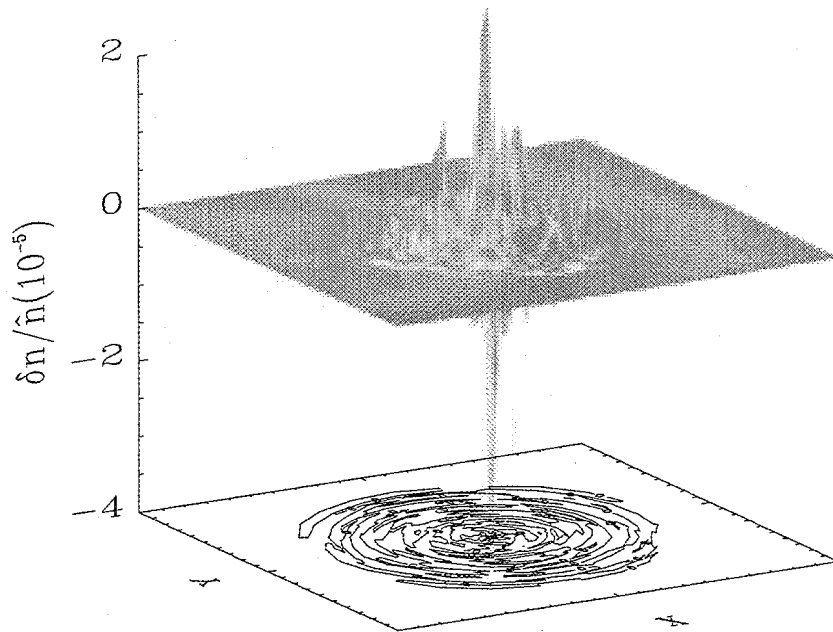


(a) Equilibrium Density

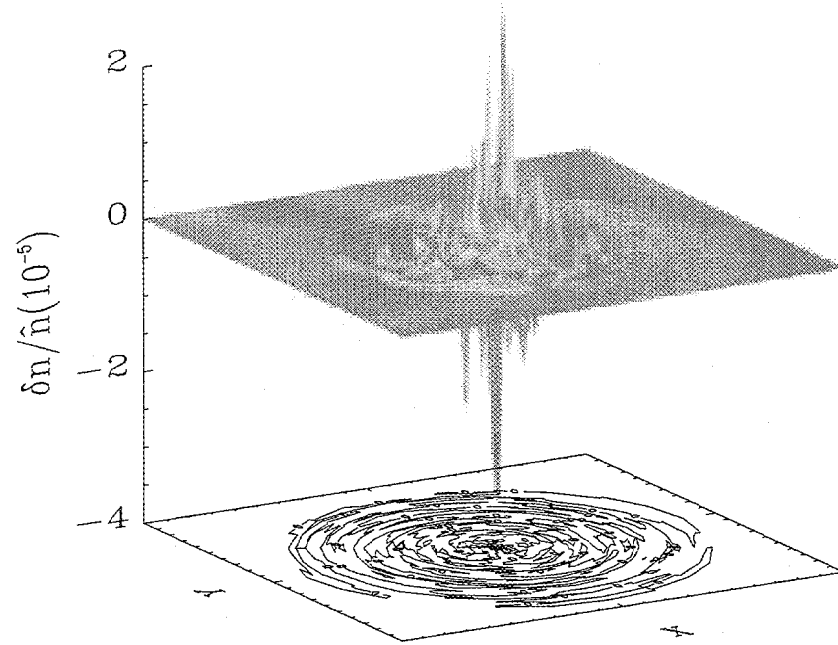


(b) Equilibrium Space-Charge Potential

⇒ Equilibrium solutions  $(\phi_0, A_{z0}, f_{j0})$  solve the steady-state  $(\partial/\partial t = 0)$  Vlasov-Maxwell equations with  $\partial/\partial z = 0$  and  $\partial/\partial \theta = 0$ .

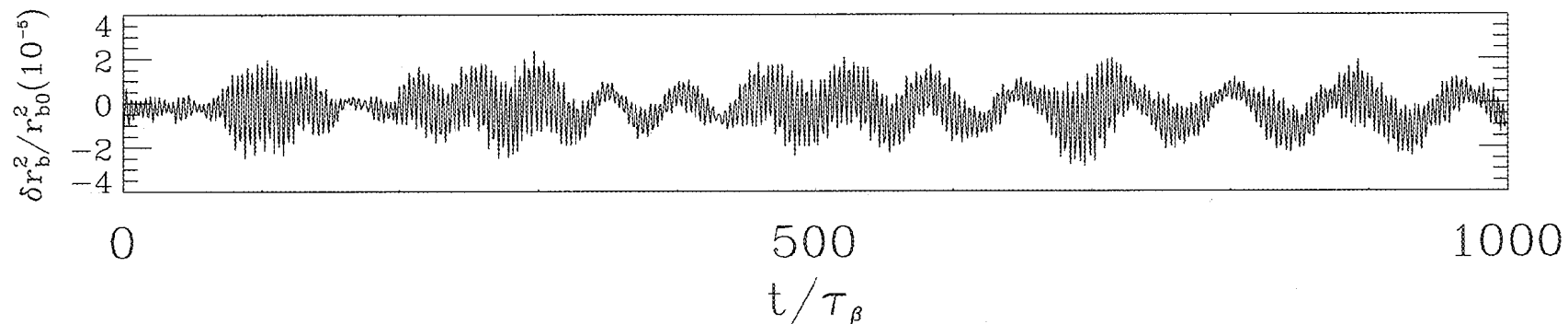
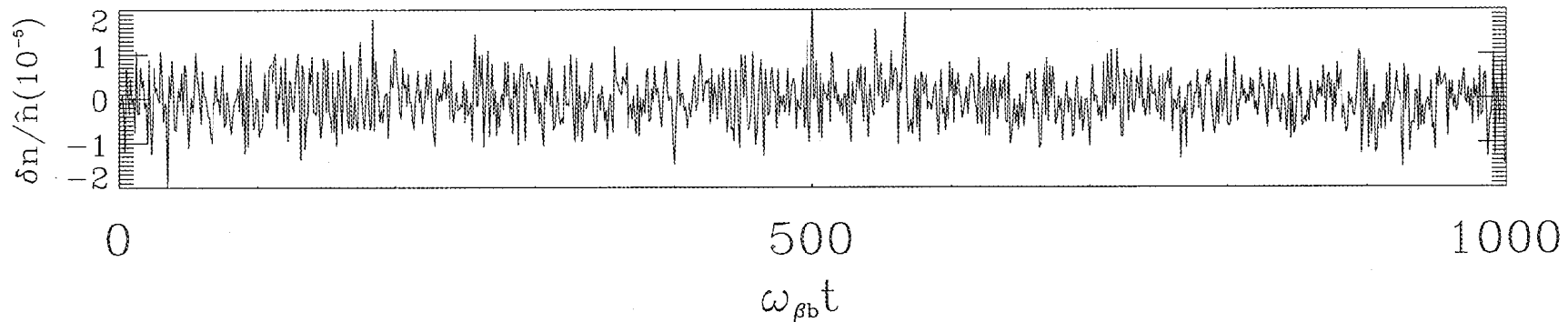


(a) Perturbed  $\delta n$  at  $t = 0\tau_\beta$ .



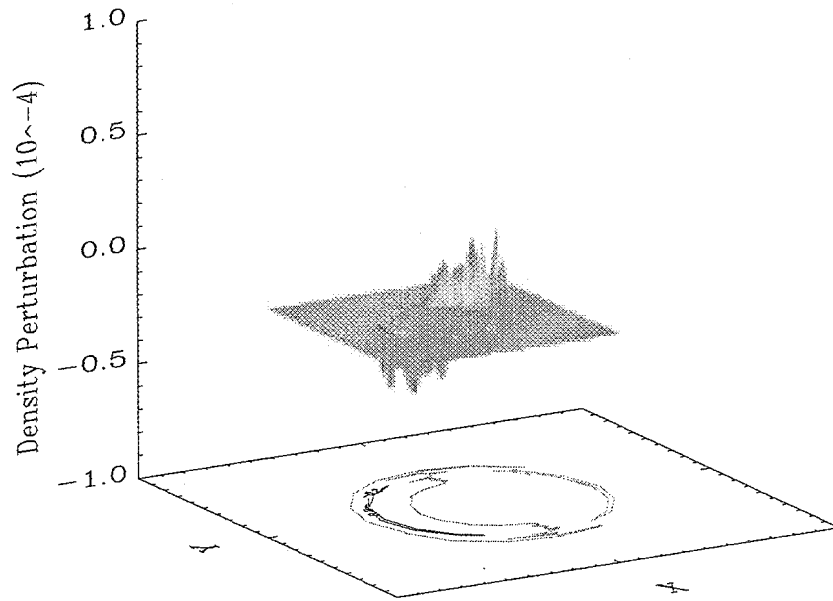
(b) Perturbed  $\delta n$  at  $t = 1000\tau_\beta$ .

- ⇒ Random initial perturbation with normalized amplitudes of  $10^{-4}$  are introduced into the system.
- ⇒ The beam is propagated from  $t = 0$  to  $t = 1000\tau_\beta$ , where  $\tau_\beta \equiv \omega_{\beta b}^{-1}$ .

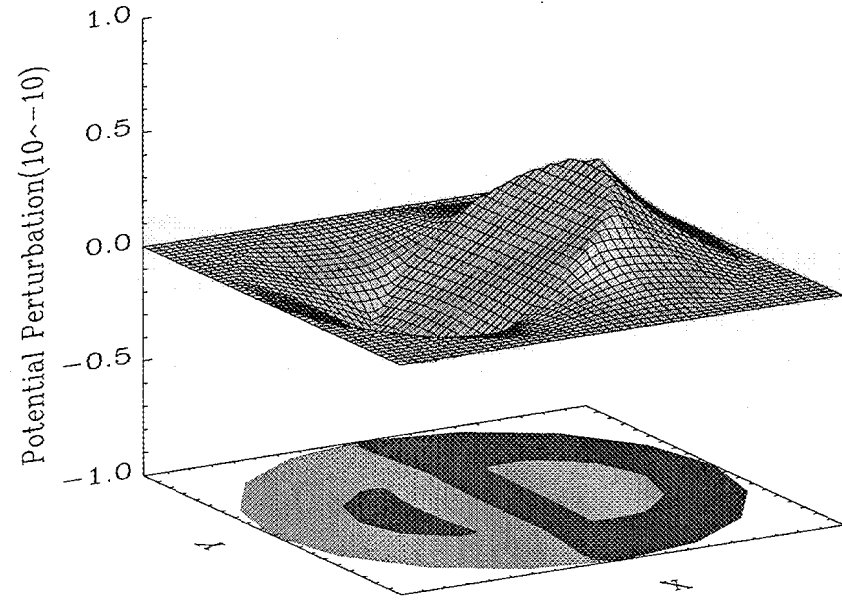


- ⇒ Simulation results show that the perturbations do not grow and the beam propagates quiescently, which agrees with the nonlinear stability theorem for the choice of thermal equilibrium distribution function.

- ⇒ These modes can be destabilized by the electron-ion two-stream interaction when background electrons are present.
- ⇒ The BEST code, operating in its linear stability mode, has recovered well-defined eigenmodes which agree with theoretical predications.



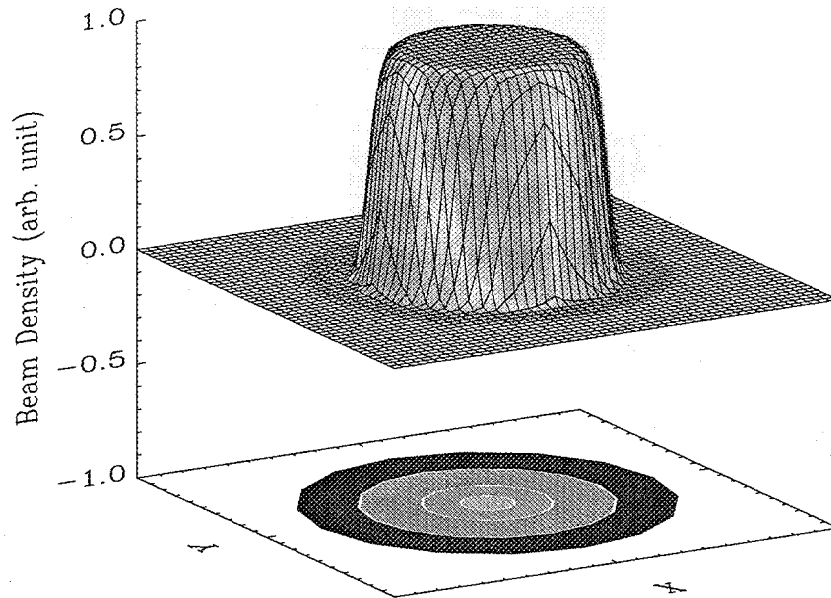
(a) Density Perturbation.



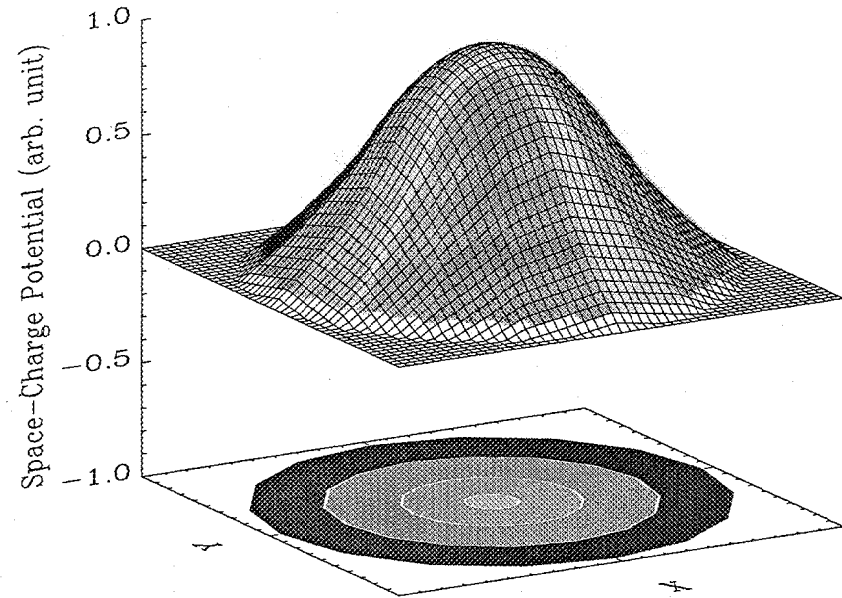
(b) Potential Perturbation.



⇒ Linear surface modes for perturbations about a thermal equilibrium beam in the space-charge-dominated regime, with flat-top density profile.



(a) Equilibrium Density



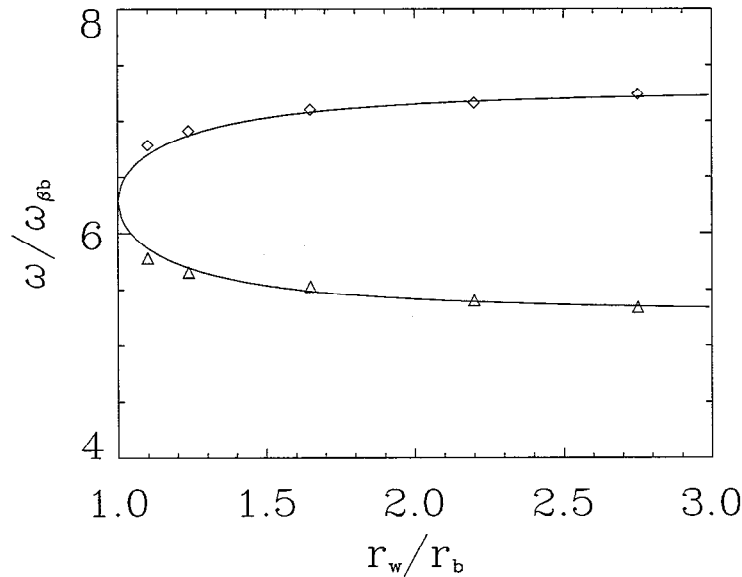
(b) Equilibrium Space-Charge Potential

⇒  $\hat{\omega}_{pb}^2 / 2\gamma_b^2 \omega_{\beta b}^2 = 0.99999995!!$

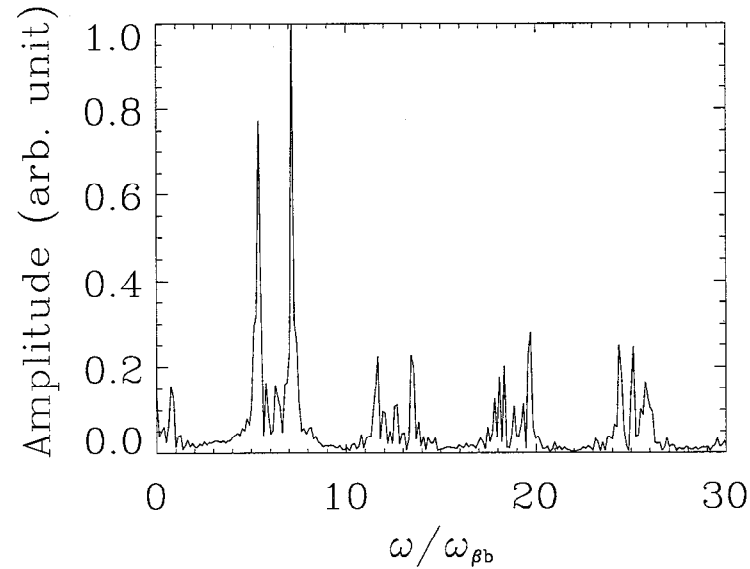
⇒ For azimuthal mode number  $l = 1$ , the dispersion relation is given by

$$\omega = k_z V_b \pm \frac{\hat{\omega}_{pb}}{\sqrt{2}\gamma_b} \sqrt{1 - \frac{r_b^2}{r_w^2}} \quad (1)$$

where  $r_b$  is the radius of the beam edge, and  $r_w$  is location of the conducting wall. Here,  $\hat{\omega}_{pb}^2 = 4\pi\hat{n}_b e_b^2 / \gamma_b m_b$  is the ion plasma frequency-squared, and  $\hat{\omega}_{pb} / \sqrt{2}\gamma_b \simeq \omega_{\beta b}$  in the space-charge-dominated limit with  $K\beta_b c \tau_{\beta} / \epsilon_0 \gg 1$ .

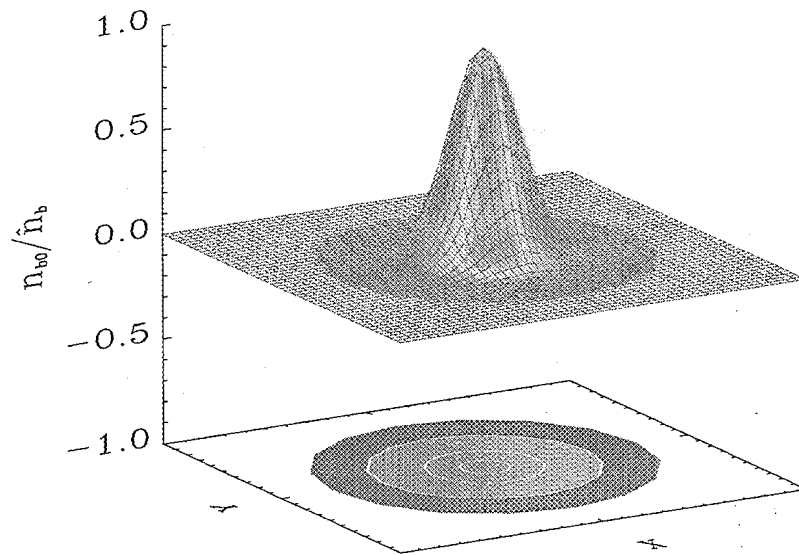


(a)  $\omega/\omega_{\beta b}$  versus  $r_w/r_b$

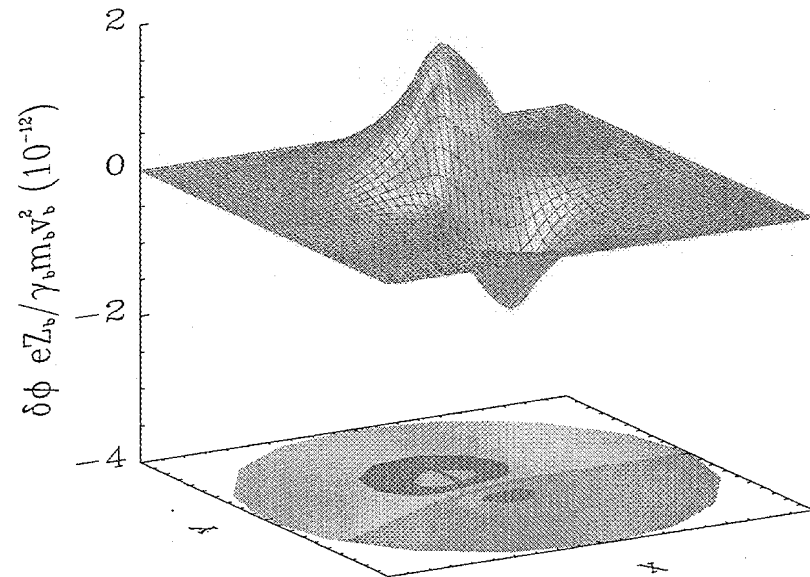


(b) Spectrum for  $r_w/r_b = 2.2$

- ⇒ Generally, there is no analytical description of the eigenmodes in beams with nonuniform density profiles.
- ⇒ However, numerical results show that the eigenmode is localized in the region where the density gradient is large.

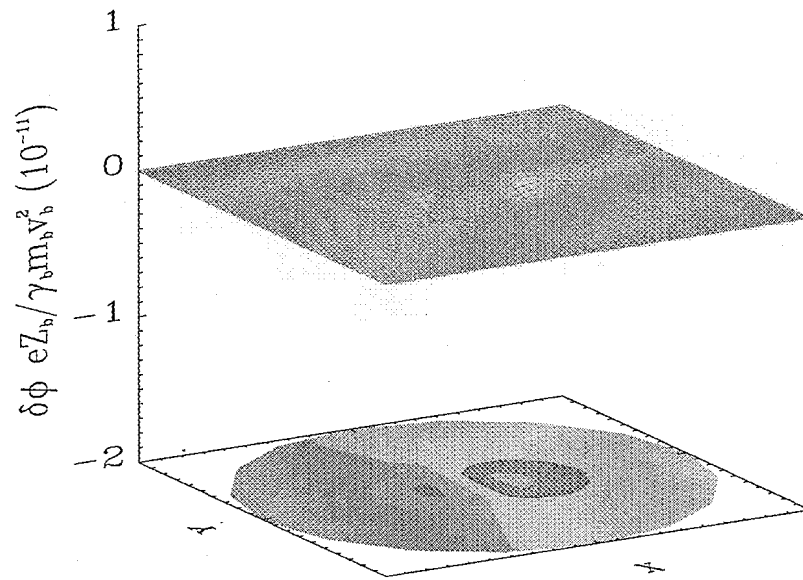


(a) Equilibrium Density Profile

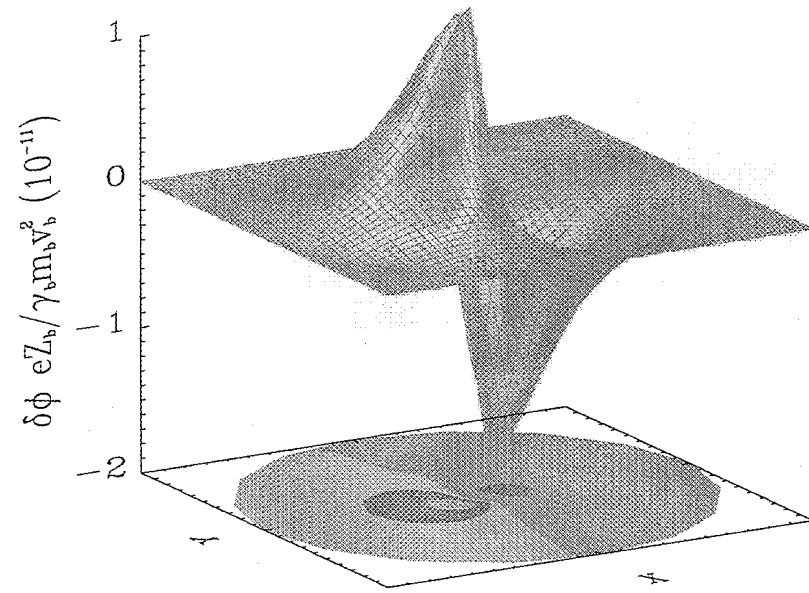


(b) Mode Structure

⇒ When a background electron component is introduced with  $\beta_e = V_e/c \simeq 0$ , the  $l = 1$  “surface mode” can be destabilized for a certain range of axial wavenumber and a certain range of electron temperature  $T_e$ .



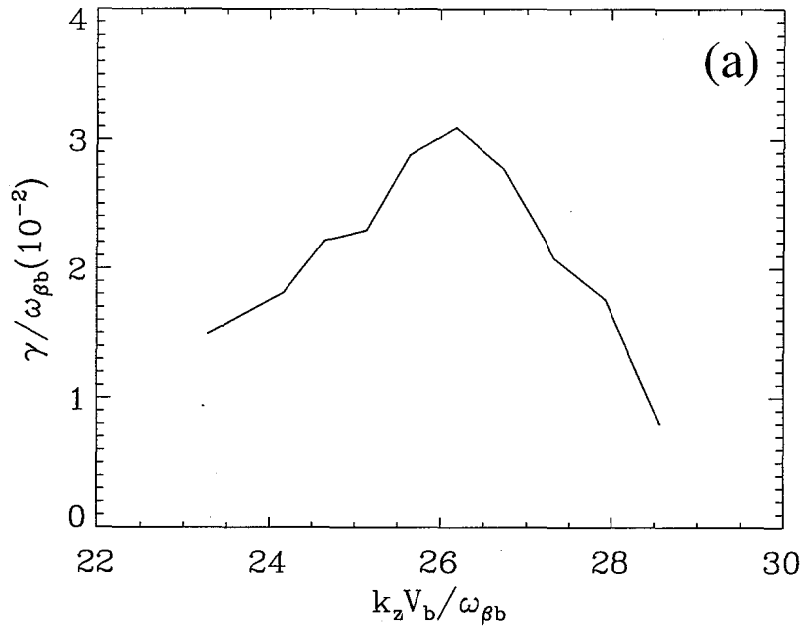
(a)  $t = 0$



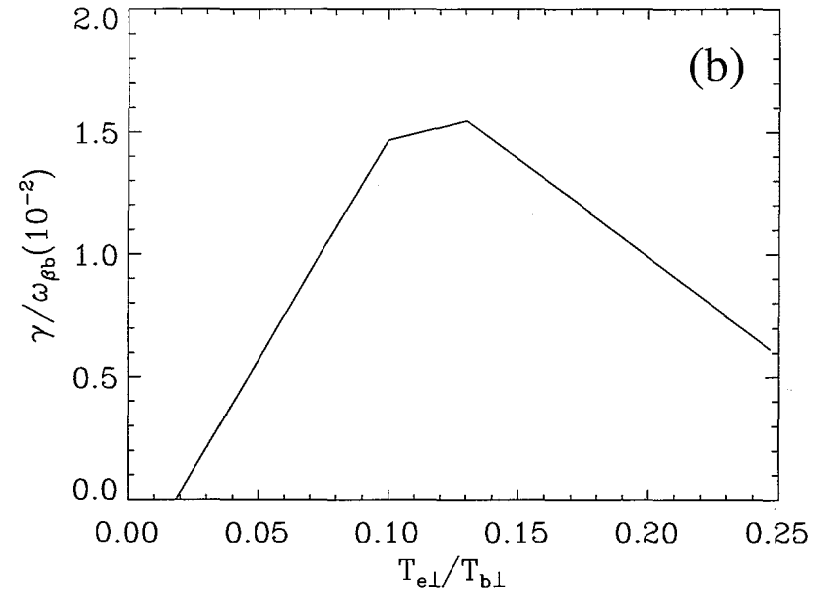
(b)  $t = 200/\omega_{\beta b}$

- ⇒ System parameters:  $\hat{\omega}_{pb}^2/2\gamma_b^2\omega_{\beta b}^2 = 0.079$ ,  $T_{b\perp}/\gamma_b m_b V_b^2 = 3.61 \times 10^{-6}$ , and  $f = \hat{n}_e/\hat{n}_b = 0.1$ . For the Proton Storage Ring (PSR) with  $\gamma_b = 1.85$ ,  $\omega_{\beta b} = 4.07 \times 10^7$ /s, the illustrative simulation parameters are:  
 $r_w = 5.0\text{cm}$ ,  $r_b = 1.7\text{cm}$ ,  $r_e = 2.15\text{cm}$ ,  $\hat{n}_b = 2.16 \times 10^8\text{cm}^{-3}$ ,  
 $N_b = 9.13 \times 10^8\text{cm}^{-1}$ ,  $N_e = 9.25 \times 10^7\text{cm}^{-1}$ ,  
 $T_{b\perp} = 4.41\text{Kev}$ ,  $T_{e\perp} = 0.73\text{Kev}$ ,  $\phi_0(r_w) - \phi_0(0) = -3.08 \times 10^3\text{Volts}$ .
- ⇒  $k_z V_b/\omega_{\beta b}$  dependence ( $k_z = 2\pi n/L = n/R$ ,  $R$  = ring radius):
- Only for a certain range of  $k_z V_b/\omega_{\beta b}$  can the collective mode of the beam ions effectively resonate with the electrons and produce instability.
- ⇒  $T_{e\perp}/T_{b\perp}$  dependence:
- For instability, electrons must physically overlap the region of the eigenmode.
  - Electrons are radially confined by the space charge potential of the beam ions.
  - Transverse electron temperature determines the radial extent of the electron density profile.

⇒ The  $k_z V_b / \omega_{\beta b}$  and  $T_{e\perp} / T_{b\perp}$  dependences of the growth rate are qualitatively consistent with the analytical results obtained for uniform-density beams.

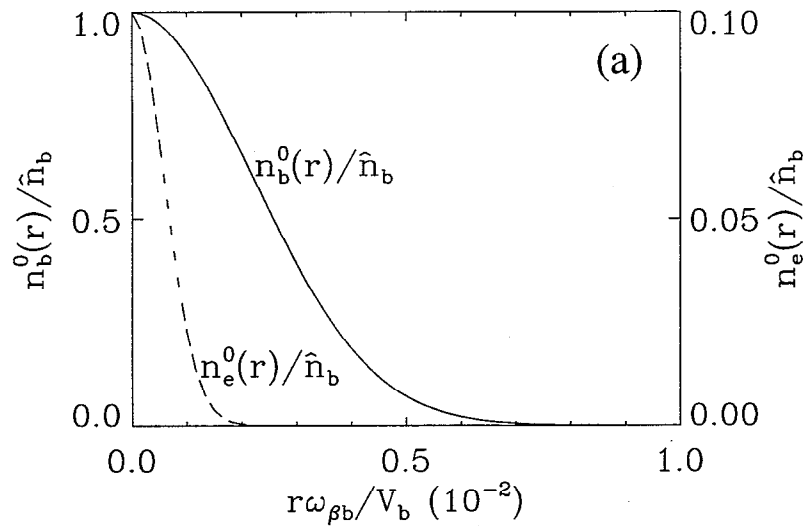


(a)  $\gamma$  versus  $k_z V_b / \omega_{\beta b}$

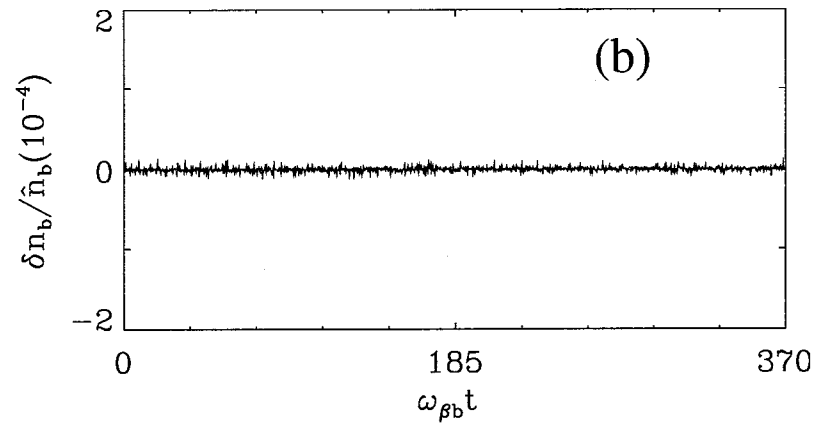


(b)  $\gamma$  versus  $T_{e\perp} / T_{b\perp}$

⇒ Electrons are relatively cold and localized in the beam center, and no instability developed over  $370\omega_{\beta b}^{-1}$ .

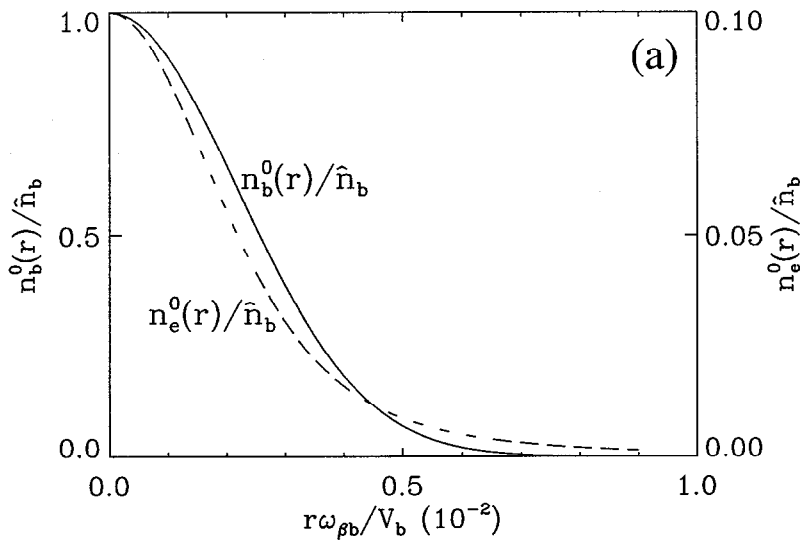


(a) Equilibrium Density

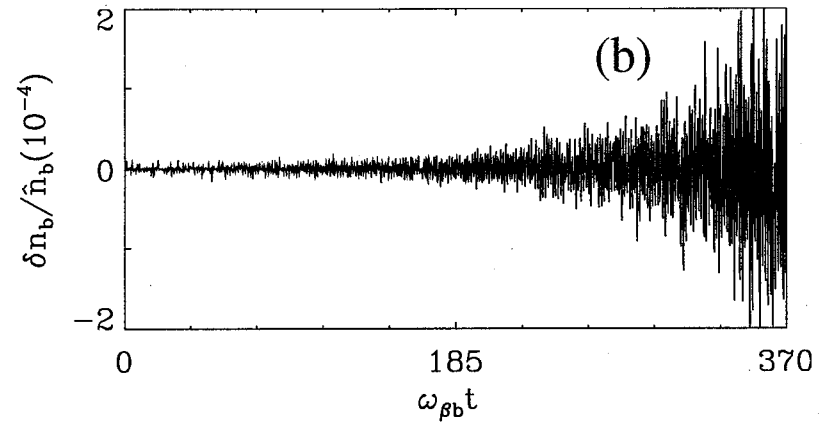


(b) Perturbation Time History

⇒ Electrons are sufficiently hot that the electron density profile overlaps that of the beam ions, and the onset of a strong e-p instability is observed.



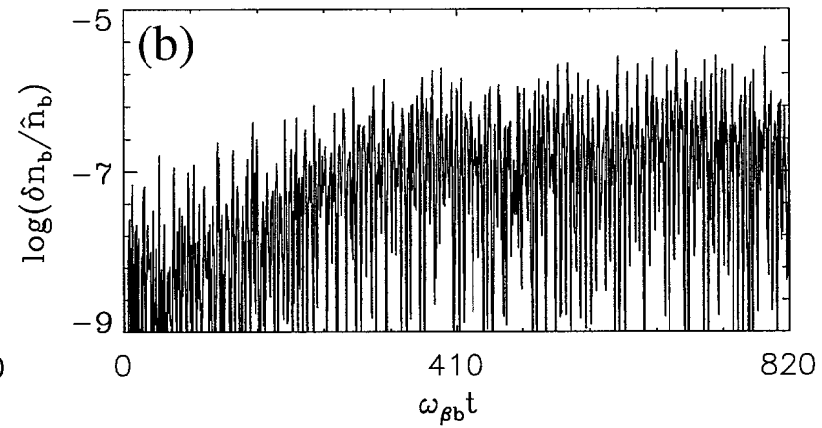
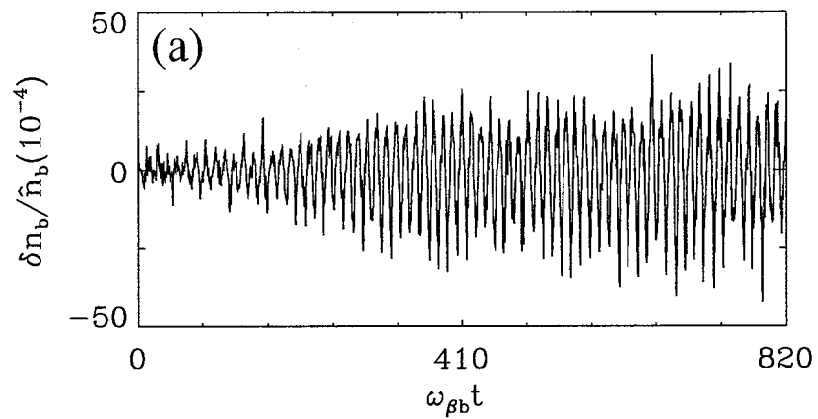
(a) Equilibrium Density



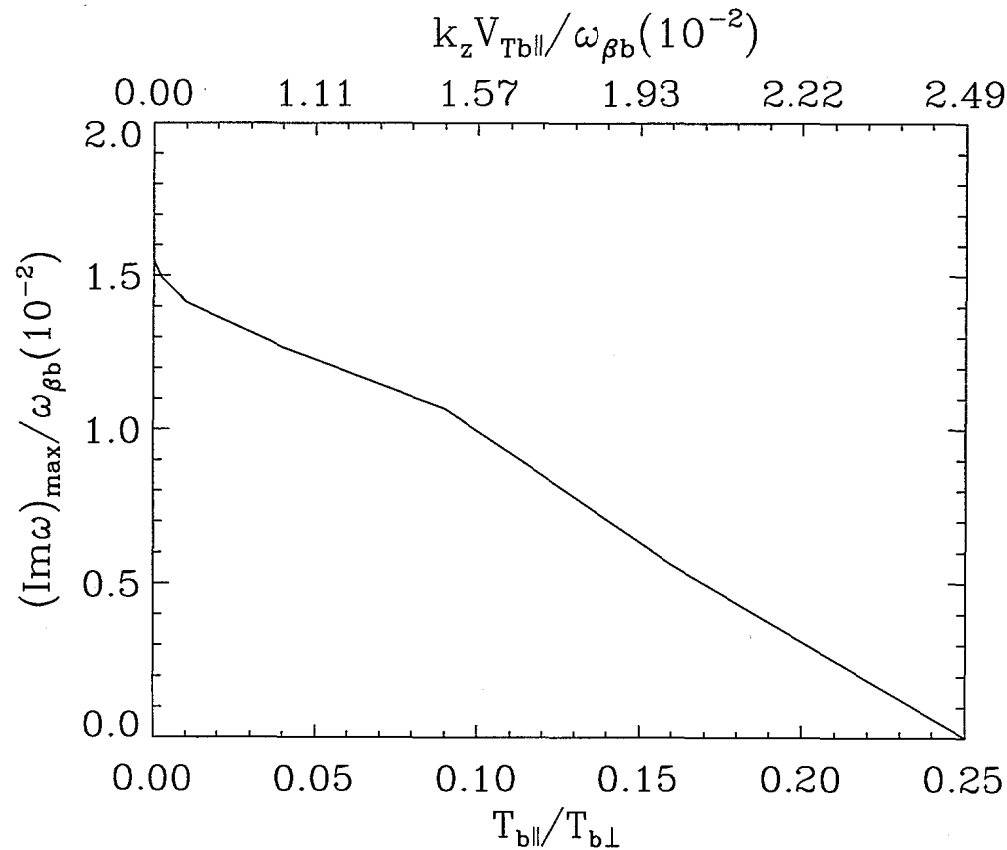
(b) Perturbation Time History



⇒ Nonlinear perturbation saturation level  $\delta n_b \sim 3.0 \times 10^{-3} \hat{n}_b = 6 \times 10^5 \text{ cm}^{-3}$ .



- ⇒ The maximum linear growth rate  $(Im\omega)_{max}$  of the electron-proton instability decreases as the axial momentum spread of the beam ions increases.



- ⇒ A 3D multispecies nonlinear perturbative particle simulation method has been developed to study two-stream instabilities in intense charged particle beams described self-consistently by the Vlasov-Maxwell equations.
- ⇒ Introducing a background component of electrons, the two-stream instability is observed in the simulations. Several properties of this instability are investigated numerically, and are found to be in qualitative agreement with theoretical predictions.
- ⇒ For PSR parameters, the simulations show that the e-p instability has a dipole mode structure, and the growth rate depends sensitively on  $T_{e\perp}/T_{b\perp}$  and the radial distribution of electrons.
- ⇒ For PSR parameters, the simulations show that an axial momentum spread provides an effective stabilization mechanism for the e-p instability.

- ⇒ The BEST code, a 3D multispecies perturbative particle simulation code, has been tested and applied in different operating regimes.
- ⇒ Simulation particles are used to follow only the perturbed distribution function and self-fields. Therefore, the simulation noise is reduced significantly.
- ⇒ Perturbative approach also enables the code to investigate different physics effects separately, as well as simultaneously.
- ⇒ The BEST code can be easily switched between linear and nonlinear operation, and used to study both linear stability properties and nonlinear beam dynamics.
- ⇒ These features provide us with an effective tool to investigate the electron-ion two-stream instability, periodically focused solutions in alternating-gradient focusing fields, halo formation, and many other important problems in nonlinear beam dynamics and accelerator physics.

- ⇒ Further studies on mode structure, thresholds, and stabilization mechanism for the two-stream instability.
- ⇒ Understand nonlinear dynamics of the two-stream instability, including mode saturation, and ion and electron dynamical response.
- ⇒ Identify illustrative operating regimes for PSR and SNS that minimize the deleterious effects of the two-stream instability and maximize the threshold beam intensity for the onset of the two-stream instability.
- ⇒ The BEST code is being parallelized to run on tera-scale parallel computers.